

Structural and morphological properties of TiO₂ thin films prepared by spray pyrolysis

N. Castillo, D. Olgún, and A. Conde-Gallardo*

*Departamento de Física, Centro de Investigación y de Estudios Avanzados del IPN,
Apartado Postal 14-740, México D.F. 07360, México*

S. Jiménez-Sandoval

*Laboratorio de Materiales, Centro de Investigación y de Estudios Avanzados del IPN, Unidad Querétaro,
Apartado Postal 1-798, Arteaga 5. Centro, 76001, Querétaro, México*

Recibido el 28 de agosto de 2003; aceptado el 26 de enero de 2004

In the present work the ultrasonic spray pyrolysis technique was employed to produce TiO₂ thin films on fused quartz and on silicon substrates. An aerosol, generated ultrasonically, of titanium diisopropoxide was employed in the deposition experiments. The crystallization process of the as deposited samples was studied by X-Ray Diffraction (XRD), Raman spectroscopy (RS), Atomic Force Microscopy (AFM), and optical transmission spectroscopies (TS). The results show that spray pyrolysis technique is able to produce films with smooth surface and good crystalline properties. When deposition temperatures were below 400°C, the films grow with a flat surface (roughness ~5Å) but in amorphous phase; while for equal or higher values to this temperature, the films develop a crystalline phase corresponding to the TiO₂ anatase phase, but the surface roughness is increased up to ~225Å. After annealing at 750°C, the samples deposited on Si show a partial transition to rutile phase preferentially oriented in (111) direction; while, under a similar annealing, those films deposited on fused quartz do not show any phase transition.

Keywords: Chemical vapor deposition; spray pyrolysis; TiO₂ thin films.

En el presente trabajo la técnica de rocío pirolítico fue empleada para producir películas delgadas de TiO₂ sobre sustratos de cuarzo y silicio cristalino (Si). Generado por ultrasonido, un aerosol de di-isopropóxido de titanio fue usado como precursor en los depósitos. El proceso de cristalización como función de los parámetros de depósito fue estudiado por difracción de rayos-X (XRD), espectroscopía Raman (RS), microscopía de fuerza atómica (AFM) y espectroscopía óptica de transmisión (TS). Los resultados demuestran que la técnica de rocío pirolítico puede producir películas con superficies planas y buenas propiedades cristalinas. Cuando la temperatura de depósito es menor a 400°C, la película crece con una superficie suave (rugosidad ~5Å) pero en una fase amorfa; sin embargo a temperaturas iguales a 400°C o mayores las películas cristalizan en la fase anatasa aun cuando la rugosidad se incrementa hasta un valor que depende del espesor. Después de un tratamiento térmico a 750°C, las muestras depositadas sobre Si muestran una transición parcial a la fase rutilo del TiO₂ con orientación preferencial (111); sin embargo, las películas depositadas sobre cuarzo no muestran tal transición.

Descriptores: Depósito en fase vapor; rocío pirolítico; películas de TiO₂.

PACS: 82.33.Ya; 81.15.Rs; 77.84.Dy

1. Introduction

The study about the growth of titanium dioxide (TiO₂) films is being increased because of the technological applications of this material [1]. Indeed; TiO₂ films can be used as coating in anticorrosive protection [2], as catalyst in chemical industry, and environmental purification phenomena [3-5]. Likewise, TiO₂ has been proposed as host matrix for luminescent devices [6] and, due to its photoelectric and photocatalytic properties, it has been proposed as photochemical converter in solar energy conversion too [3,7-9]. Furthermore, considering its high dielectric constant, this inorganic metal oxide is being strongly considered to replace the SiO₂ in the metal-oxide-semiconductor gates in the microelectronic industry [1,10]. In most of these applications, films with good crystalline and flat surface properties are required. Because of this, new ways of developing TiO₂ films with the required quality are always explored. Thus, rf-sputtering, sol-gel, chemical vapor deposition (CVD), plasma enhanced CVD, atomic layer deposition, and spray pyrolysis

are some techniques that have been used to produce titanium dioxide films [11-17]. In particular, we are interested in exploring the spray pyrolysis (SP) deposition technique to produce TiO₂ films and compare it with the CVD technique.

In the CVD technique, the precursor compounds that constitute the solid film, impinges on the substrate in a true vapor phase in such a way that a reaction can take place as soon as (or even before) the substrate surface is reached [18]. In the SP technique, usually, a set of liquid droplets splash the substrate, and immediately the temperature evaporates the residual solvents leaving a dry precipitate and a chemical reaction follows. However, whether or not the initial droplets really splash the substrate, depends on the thermodynamic properties of the source solution containing the metallic precursors [18-20]. Indeed, if the droplets are evaporated before they reach the substrate surface, the SP technique could give place to a growth process similar to that found in the CVD. This approach to CVD from SP, can be promoted if instead of using a pneumatic nebulization to produce the droplets, they are generated ultrasonically [21]. Such method reduces the

TABLE I. Deposition conditions and physical properties of TiO₂ anatase films deposited on Si and fused quartz substrates.

SAMPLE	SUBSTRATE	SUBSTRATE TEMPERATURE (°C) T _s	THICKNESS (nm)	Energy Gap (eV)	SURFACE ROUGHNESS (Å)
S1	Si	250	94	-	5.3
S2	Si	400	89	-	20.4
S3	Si	500	95	-	225.5
S4	Quartz	250	119	2.99	
S5	Quartz	400	92	3.30	
S6	Quartz	500	132	3.32	
S7	Si	250	225	-	
S8	Si	300	258	-	
S9	Si	500	650		224

droplets size and allows to control their homogeneity, improving in this way the pyrolysis phenomena during the deposition.

Recently, taking into account the noble evaporation properties of isopropoxide compounds, CVD technique has been used to grow TiO₂ films from titanium isopropoxide, and tetraisopropoxide as precursors [15,22]. In the present work we show that, good quality TiO₂ thin films can be obtained by spraying an aerosol of titanium diisopropoxide on fused quartz and crystalline silicon (100) substrates.

2. Experimental details

The growth process by spraying an aerosol generated ultrasonically, has been described elsewhere [18-21]. In the present work, an ultrasonic generator working at a frequency of 0.8 MHz was used. It produces droplets of 1-5 μm in average size [21]. The source of the aerosol was prepared from an ethanol diluted Titanium diisopropoxide solution in a proportion of 4:1 in volume. Oxygen was used as carrier gas to conduct (through a glass nozzle 12 mm in diameter) the aerosol to the substrate. The flux of this gas was fixed at a constant value of 3.5 l/min. Two kinds of substrates were used: crystalline silicon oriented in the (100) direction, and amorphous fused quartz. The studied samples and their deposition conditions are reported in Table I. Various substrate temperatures (T_s) were used. By regulating the deposition time the films thickness were controlled at an average deposition rate of 60 nm/min. However, it is evident that this deposition rate depends strongly on the concentration of the starting solution; in the present study the concentration was kept constant. Pieces of samples were post annealed at 650°C and 750°C in an oxygen flux atmosphere. The crystallization process was examined by a standard X-ray powder diffractometer (CuK α = 1.5418 Å), and confirmed by Raman spectroscopy. The surface morphology was evaluated by atomic force microscopy (AFM). In this last technique, the images were verified by scanning in both x and y directions in the tapping mode (\sim 13 nN), avoiding in this way drift effects. By

stepping the samples, this technique was also used to measure the films thickness. UV visible reflectivity and transmission spectroscopies were performed with a UNICAM 8700 spectrometer in the 200-900 nm wavelength range and with 1 nm resolution. These spectroscopies were used too to confirm, through interference effects, the films thickness.

3. Results and discussion

Even after months, films show good adherence to the substrates. Figure 1 shows the x-ray diffraction (XRD) for three samples deposited on Si at different temperatures. For substrate temperatures below 400°C, besides the signal coming from the substrate, no indication of crystallization is observed; while for temperatures equal or above this T_s value, a clear signal of diffraction peaks appears. Similar behavior was observed for films deposited on fused quartz substrates; in the inset of Fig. 1c, besides the broad signal coming from the amorphous substrate, diffraction peaks are well defined for a film deposited at T_s=500°C. The more intense peaks are identified with TiO₂ anatase phase; but traces of an extra phase are found, as far as the presence of a small peak at $2\theta=41.20^\circ$ reveals. The evolution of the crystallization process observed by XRD is also confirmed by the Raman spectroscopy, Fig. 2. The E_g(1) \sim 145, B_{1g}(1) \sim 398, and E_g(3) \sim 662 cm⁻¹ Raman active modes [21-22] are more defined as the substrate temperature increases. In particular, the characteristic E_g(1) mode of anatase phase increases as the crystalline phase does. A significant confirmation of the evolution observed by XRD, and Raman is obtained by AFM experiments, Fig. 3. Samples deposited at 250°C (Fig. 3a and Fig. 3b) develop smooth surfaces; however, indication of grains with a defined morphology appears when the temperature of the deposition is fixed equal or higher to 400°C, Figs. 3c-3d. It is important to say that for scanned areas smaller than those shown in the Fig. 3, no signal of crystalline surface was detected for samples deposited at 250°C; indicating that, and in total agreement with the x-ray diffraction results, a true amorphous surface phase is developed for

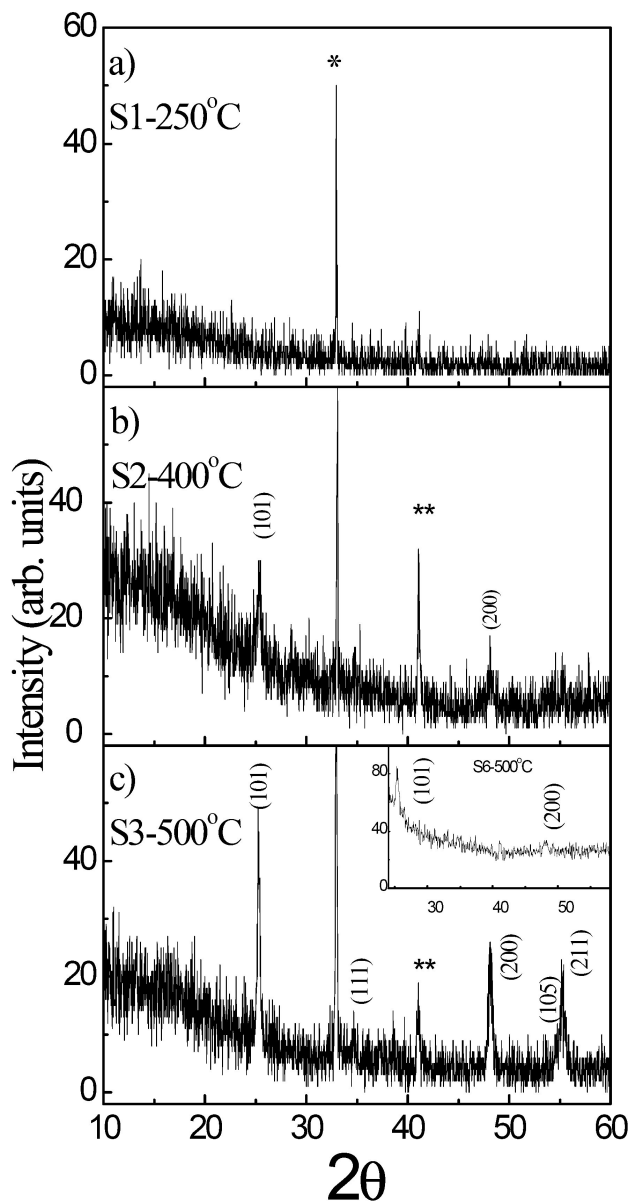


FIGURE 1. X-ray diffraction of TiO₂ films deposited at various substrate temperatures. The indexed peaks correspond to TiO₂ anatase phase. Peak (*) belong to the Si substrate. The peak (**) is associated to the (111) plane of the rutile phase (see the text). The inset correspond to a film deposited on amorphous fused quartz substrate (S6).

these deposition parameters. For $T_s=500^\circ\text{C}$, the surface morphology suggests that the grains grow in a more irregular form, as can be observed directly in Fig. 3e-3f, and by the surface roughness values reported in Table I. From the AFM images, an average grain size $\sim 0.05\mu$ can be deduced for those films deposited at $T_s=500^\circ\text{C}$; in total agreement with average grain size ($\sim 400\text{\AA}$) obtained by the Scherrer equation applied to the diffraction peaks of Fig. 1c. However XRD indicates smaller grains size for the sample S2; suggesting that those grains observed in Fig. 3c-3d are not single crystals. Even though a higher surface roughness was observed for thicker films deposited under same conditions (samples S7-S9 in Ta-

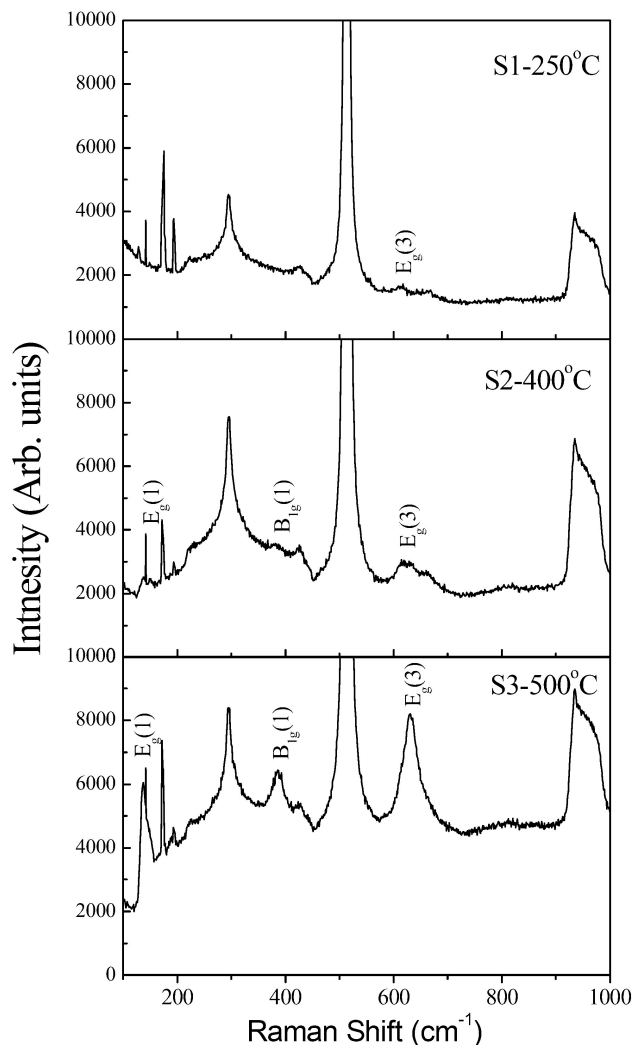


FIGURE 2. Raman Spectroscopy for the samples S1, S2 and S3.

ble D), they have a crystalline behavior similar to that shown in Fig. 1. This means that the kinetic of the deposition of TiO₂ anatase phase by spraying an aerosol of titanium diisopropoxide, is mainly determined by the substrate temperature rather than by a critical thickness. From all this and in as much as no trace of splashing process was observed even for thinner films, it can be concluded that this growth process is rather close to CVD than to the classical spray pyrolysis; where usually the splashing process (flattening and spreading out) of the droplets determines the surface quality. In this regard, titanium diisopropoxide behaves like titanium acetylacetonate, already used as source material to grow TiO₂ thin films by SP [16-17]. However, the surface morphology and the grain size of the present films are different as they are compared with those deposited from acetylacetonates. The differences must be related with the decomposition process of those starting materials. Indeed, in the present case no perceptible changes, as function of T_s , were observed in the deposition rate (similar film thickness S1-S3 or S4-S6 were obtained during similar deposition time). Likewise, and even though that in the present study higher deposition rates were

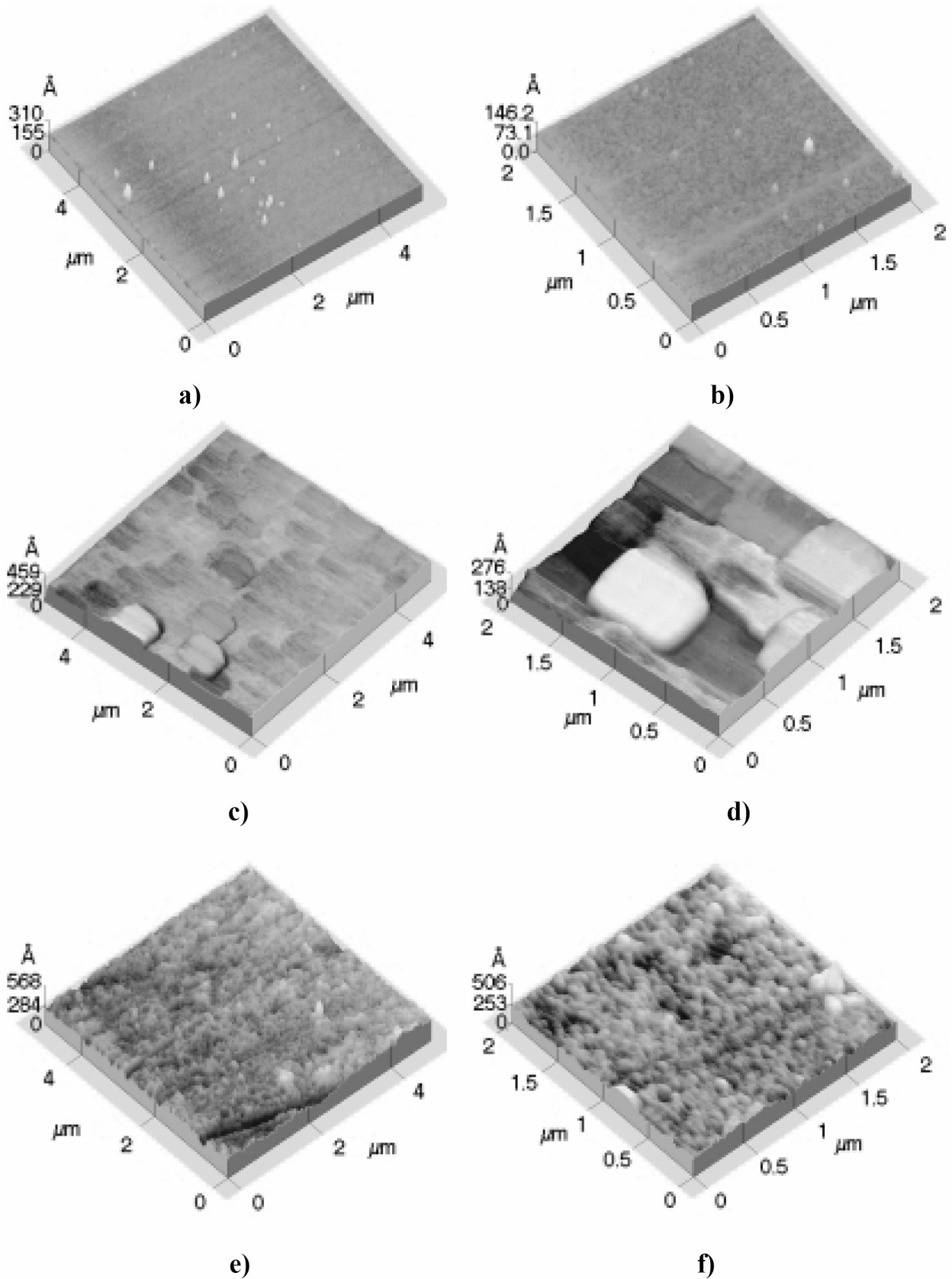


FIGURE 3. AFM images of films deposited at various substrate temperatures. Two scanned areas are shown. (a)-(b) $T_s = 250^\circ\text{C}$, (c)-(d) $T_s = 400^\circ\text{C}$ and (e)-(f) $T_s = 500^\circ\text{C}$.

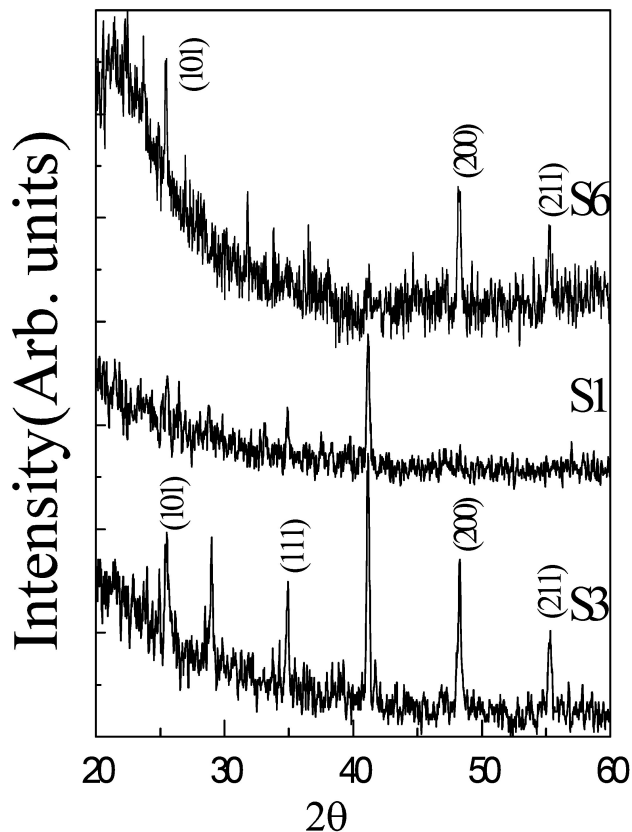


FIGURE 4. X-ray diffraction of samples S1, S3 and S6 after annealing at 750°C.

used as compared with those used in the Ref. 17, the surface roughness of our films does not decrease as function of T_s but, the other way around, it is increased. Similar effects have been observed when films are deposited by CVD using similar precursors [15]. A major difference is found in the phase transformation during a post isothermal annealing. As can be observed in Fig. 4, after an annealing at 750°C the TiO₂-anatase film deposited on Si substrates is transformed to other crystalline phase. The presence of a strong peak at $2\theta = 41.20^\circ$ means that this corresponds to a (111) TiO₂-rutile oriented film. Nevertheless, it is important to observe that for those films deposited on fused quartz substrates (S6), no phase transition is detected, but just the anatase phase is defined in a better way. Even more, it is worth noting that the evolution in TiO₂/Si films depends on the initial order-disorder arrangement in which the atoms are before the annealing. While a nice $2\theta = 41.20^\circ$ orientated peak is obtained for an initially amorphous films (S1), no complete phase transformation is observed for films in an initially crystalline phase (S3). These differences in the mechanism of phase transformation must be associated with the diffusion length of the atoms in each initial phase. The process is still unclear. It is under study and will be reported elsewhere.

Finally, Fig. 5 shows the absorption coefficient of the as deposited films, on the optically transparent fused quartz substrates. The coefficient was calculated from transmittance experiments by the rough approximation $\alpha = -\ln(T)/d$, valid in

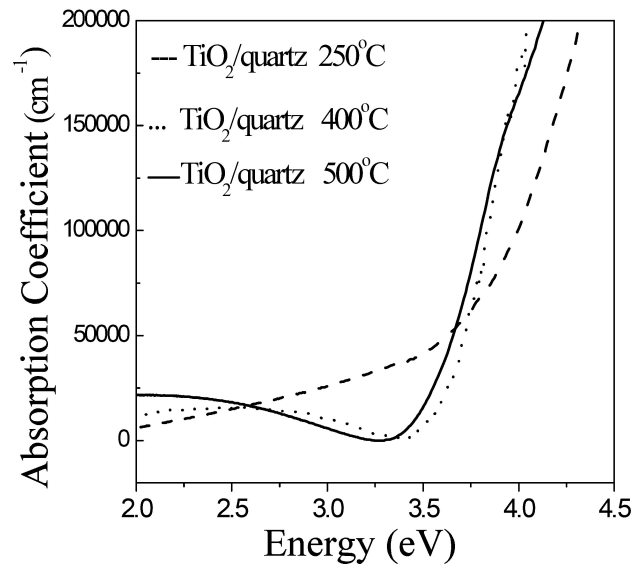


FIGURE 5. Optical absorption coefficient for the samples S4, S5 and S6 deposited on fused quartz substrates. The straight lines represent the fitting to the equation $\alpha^{1/2} = (h\nu - E_g)$

the strong absorption region (near the band gap) [25]. As expected, the absorption changes as function of the crystalline properties. Considerable defect levels inside the band gap make the optical absorption so broad for the amorphous phase; while a rather sharp behavior is observed for those films with a crystalline structure. Considering the equation $\alpha = (h\nu - E_g)^2$, suitable for indirect optical transitions, it is possible to evaluate the optical band gap E_g for those films, see Table I. Probably due to our rough approximation in the way of getting the α vs $h\nu$ curve, the E_g values for the present TiO₂ anatase films are slightly higher than those measured for single crystals [26-28]; even though, an alternative explanation could be the induced stress effects caused by the mismatch between the films and the substrates.

4. Conclusions

TiO₂ thin films with smooth surface and good crystalline quality have been obtained through the spray pyrolysis of an aerosol, generated ultrasonically, of titanium diisopropoxide. From the analysis of the crystalline properties, and surface roughness of the as deposited films, it can be concluded that the growth process is near as to a chemical vapor deposition than to the typical splashing mechanisms of spray pyrolysis. At low deposition temperatures, the films grow in amorphous phase. When T_s is fixed at 400°C or higher values, they start to crystallize in the anatase phase. The developed surface have roughness values in the range of 5-225Å depending on the deposition temperature. A crystalline phase transition starts when the samples deposited on silicon substrates are post annealed at 750°C, but not such phase transformation takes place for those films deposited on fused quartz substrates. The band gap values, determined by transmission spectroscopy, change according to the crystalline state of the

films, and they are slightly higher than those reported for single crystals of TiO₂-anatase phase.

Acknowledgements

This work was partially supported by the National Council for Science and Technology in Mexico (CONACyT 34391-E).

-
- * Corresponding Author: Phone: (525) 5061 3800 X 6168, Fax: (525) 5754 7096, e-mail:aconde@fis.cinvestav.mx
1. Ulrike Diebold, *Surf. Sci. Rep.* **48** (2003) 53.
 2. T. Honda *et al.*, *Jpn. J. Appl. Phys.* **33** (1994) 3960.
 3. A.L. Linsebigler, G. Lu, and J.T. Yates, Jr. *Chem. Rev.* **95** (1995) 735.
 4. Xiao-Ping Wang, Yun Yu, Xing-Fang Hu, and Lian Gao, *Thin Solid Films* **317** (2000) 148.
 5. P.C. Maness, S. Smolinski, and W.A. Jacoby, *Appl. Environ. Microbiol.* **65** (1999) 4094.
 6. A. Conde-Gallardo, M. García-Rocha, I. Hernández-Calderón, and R. Palomino-Merino, *Appl. Phys. Lett.* **78** (2001) 3436.
 7. A. Fujishima and K. Honda, *Nature* **238** (1972) 37.
 8. B. O' Regan and M. Grätzel, *Nature* **353** (1991) 737.
 9. L. Kavan, M. Grätzel, S.E. Gilbert, C. Klemenz, and H.J. Scheel, *J. Am. Chem. Soc.* **118** (1996) 6716.
 10. S.A. Campbell *et al.*, *IBM J. Res. Develop.* **43** (1999) 383.
 11. J. M. Bennett *et al.*, *Appl. Opt.* **28** (1989) 3303.
 12. J. Aarik, A. Aidla, H. Mändar, and V. Sammelselg, *J. Cryst. Growth* **220** (2000) 531.
 13. C. Legrand-Buscema, C. Malibert, and S. Bach, *Thin Solid Films* **418** (2002) 79.
 14. Li-Jian Meng and M.P. dos Santos, *Thin Solid Films* **226** (1993) 22.
 15. G.A. Battiston *et al.*, *Thin Solid Films* **371** (2000) 126.
 16. Wen Wen Xli, R. Kershaw, K Dwight, and A. Wold, *Mat. Res. Bull.* **25** (1990) 1385.
 17. L. Castañeda, J.C. Alonso, A. Ortiz, E. Andrade, J.M. Saniger, and J.G. Bañuelos, *Mat. Chem. and Phys.* **77** (2002) 938.
 18. J.C. Viguie and J. Spitz, *J. Electrochem. Soc.* **122** (1975) 585.
 19. M. Jergel, A. Conde-Gallardo, M. García, C. Falcony, and M. Jergel, *Thin Solid Films* **305** (1997) 210.
 20. M. Jergel, M. García, A. Conde-Gallardo, C. Falcony, M. A. Canseco, and G. Plesch, *Thin Solid Films* **305** (1997) 157.
 21. M. Langlet and J.C. Joubert, *Chemistry of Advanced Materials* ed. by C.N.R. Rao (Blackwell; Oxford, 1993).
 22. A. Sandell *et al.*, *J. Appl. Phys.* **92** (2002) 3381.
 23. T. Sekiya, S. Ohta, and S. Kurita, *Int. J. Mod. Phys. B* **15** (2201) 3952.
 24. M. Mikami, S. Nakamura, O. Kitao, and H. Arakawa, *Phys. Rev. B* **66** (2002) 155213.
 25. J.I. Pankove. *Optical Process in Semiconductors* (Dover Publications Inc. New York, 1975).
 26. Shang-Di Mo and W.Y. Ching, *Phys Rev. B* **51** (1995) 13023.
 27. H. Tang, K. Prasad, R. Samjinés, P.E. Schmid, and F. Lévy, *J. Appl Phys.* **75** (1994) 2042.
 28. H. Tang, H. Berger, P.E. Schmid, F. Lévy, and G. Burri, *Solid State Commun.* **87** (1993) 847.